Sensors and Actuators B 150 (2010) 226–229

Contents lists available at ScienceDirect

Sensors and Actuators B: Chemical

journal homepage: www.elsevier.com/locate/snb

Fiber Bragg grating-based fiber sensor for simultaneous measurement of refractive index and temperature

Hongyun Meng*, Wei Shen, Guanbin Zhang, Chunhua Tan, Xuguang Huang

Laboratory of Photonic Information Technology, School for Information and Optoelectronic Science and Engineering, South China Normal University, Guangzhou 510006, PR China

ARTICLE INFO

Article history:
Received 12 February 2010
Received in revised form 3 July 2010
Accepted 6 July 2010
Available online 17 July 2010

Keywords:
Fiber sensor
Fiber Bragg grating
Refractive index
Fresnel reflection
Side mode suppression ratio

ABSTRACT

A simple sensor for simultaneous measurement of refractive index and temperature in solutions based on fiber Bragg grating (FBG) is proposed. The sensor contains only a normal FBG with a pigtail fiber. When the FBG is immersed in different liquids of refractive index, the side mode suppression ratio of the FBG varies due to the Fresnel reflection of the pigtail fiber. The sensor is also capable of simultaneous measurement refractive index and temperature combining the thermo-optic effect of the FBG. Its ease of fabrication and low-cost offer the attractive applications in chemical and biological sensing.

1. Introduction

The fiber Bragg grating sensors have become an enabling sensing technology due to many of their desirable advantages such as the small size, the high sensitivity, absolute measurement capability, immunity to electromagnetic interference, wavelength multiplexing, and the suitability for remote sensing [1,2]. Thus far, the FBG sensors' capability to measure physical quantities such as temperature, strain, and pressure, has been studying extensively. However, the use of FBG sensors for the detection of environmental refractive index change has not been fully explored, due to the Bragg wavelength independence on the refractive index of ambient solution. To address the above limitation, there are several approaches proposed: the first is removing the fiber cladding to increase the evanescent field interaction with the surrounding environment, including the D-shaped fiber [3], side-polished fiber [4–7], microstructured FBG [8] and FFPI sensor [9–11], the second one is using the special fiber grating [12,13]. In the first case, the strength and durability of the sensor were greatly reduced. The special fiber grating was needed in the second one, which would raise the costs and limit the possible applications.

In this letter, we first demonstrate a simple sensor based on a normal FBG for simultaneous measurement of the refractive index and temperature in solution. Owing to the Fresnel reflection at the distal end of the pigtail fiber of the FBG, the side mode suppression ratio (SMSR) of the FBG varies with the refractive index of the solutions, and it is possible to simultaneously measure refractive index and temperature combining the thermo-optic effect of the FBG. Previously Silva et al. [10] have demonstrated a low-finesse Fabry–Perot interferometer based on the reflection of a short fiber Bragg grating and the Fresnel reflection from the cleaved fiber end. In this scheme, the two interfering waves are obtained from the Fresnel reflection at the distal end of the fiber and the reflected light from the FBG. However, in our work, the two incoherent waves are obtained from the Fresnel reflection and the FBG because the coherence length of the light source is shorter than the distance between the FBG and the distal end of the pigtail fiber.

2. Principle of operation

Fig. 1 shows the schematic of the refractive index and temperature simultaneous measurement sensor, which includes an amplified spontaneous emission (ASE) optical source as a broadband source (BBS), a circulator, a FBG and an optical spectrum analyzer (OSA). The Fresnel reflection at the distal end of the pigtail fiber taken into account, the SMSR of the FBG will vary with the refractive index of solutions. For the FBG, the full reflectivity R_{FBG} can be given by

$$R_{\mathrm{FBG}}(\lambda) = \frac{\sinh^2[\eta(V)\delta n\sqrt{1-\Gamma^2}N\Lambda/\lambda]}{\cosh^2[\eta(V)\delta n\sqrt{1-\Gamma^2}N\Lambda/\lambda]-\Gamma^2}, \quad (1)$$

* Corresponding author. Tel.: +86 2039310085; fax: +86 2039310085.
E-mail address: hymeng@scnu.edu.cn (H. Meng).

0925-4005/$ – see front matter
doi:10.1016/j.snb.2010.07.010

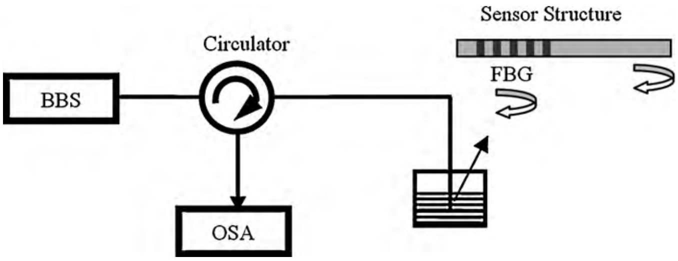

Fig. 1. Schematic diagram of the measurement system. The sensor structure is shown in the top right-hand corner.

where

$$\Gamma(\lambda) = \frac{1}{\eta(\lambda)\delta n}\left[\frac{\lambda}{\lambda_B} - 1\right], \tag{2}$$

λ_B is the Bragg wavelength, δn is the variation of the refractive index in the fiber core, Λ is the grating period, and N is the number of the periodic variations. When the wavelength is far from the Bragg wavelength, $R_{\rm FBG}(\lambda) \ll R_{\rm FBG}(\lambda_B)$. The Fresnel reflectivity at the distal end of the pigtail fiber can be given by

$$R_F = \left(\frac{n_f - n_x}{n_f + n_x}\right)^2, \tag{3}$$

where n_f is the refractive index of the fiber core, and n_x is the refractive index of the solution. Within the bandwidth of the source, the dependence of n_f and n_x on wavelength can be ignored.

When the distance between the FBG and the distal end of the pigtail fiber is longer than the coherence length of the optical source, the reflective intensity at the Bragg wavelength can be given by

$$I_{\rm out}(\lambda_B) = R_{\rm FBG}(\lambda_B)I_{\rm in} + [1 - R_{\rm FBG}(\lambda_B)]^2 R_F I_{\rm in} \approx R_{\rm FBG}(\lambda_B)I_{\rm in}. \tag{4}$$

The reflective intensity at the wavelength far from the Bragg wavelength is given by

$$I_{\rm out}(\lambda) = R_{\rm FBG}(\lambda)I_{\rm in} + [1 - R_{\rm FBG}(\lambda)]^2 R_F I_{\rm in}, \tag{5}$$

where $I_{\rm in}$ is the input intensity. The SMSR of the FBG is given by

$$\begin{aligned}\mathrm{SMSR} &= 10\log_{10}\left[\frac{I_{\rm out}(\lambda_B)}{I_{\rm out}(\lambda)}\right] \\ &= 10\log_{10}\left\{\frac{R_{\rm FBG}(\lambda_B) + [1 - R_{\rm FBG}(\lambda_B)^2]R_F}{R_{\rm FBG}(\lambda) + [1 - R_{\rm FBG}(\lambda)]^2 R_F}\right\}.\end{aligned} \tag{6}$$

When $R_{\rm FBG}(\lambda) \approx 0$ and $R_{\rm FBG}(\lambda_B)$ is sufficiently high

$$\mathrm{SMSR} = 10\log_{10}\left[\frac{R_{\rm FBG}(\lambda_B)}{R_F}\right]. \tag{7}$$

The effective index n_f of the fiber mode can be calculated from the known fiber group index n_g and the dispersion relation. The given value for n_f is 1.44961 at the wavelength of 1550 nm [14]. With Eq. (6) or (7), the value of refractive index n_x can be calculated from the measured value of SMSR.

3. Results and discussion

To validate the technique, experiments are performed with the setup shown in Fig. 1. The Bragg wavelength of the FBG is 1536.36 nm with a reflectivity of 60% at the peak and the 3-dB bandwidth of 0.15 nm. The insert loss of the circulator is 0.5 dB. The distance between the FBG center and the distal end of the pigtail fiber is 3 cm. We put the sensor in sugar solutions with different concentrations and measure the reflectivity of the FBG through scanning the wavelength with an optical spectrum analyzer. The reflection spectral responses to the FBG sensor in air (n = 1.000), pure water (n = 1.3119) and the sugar solutions with the concentrations of 12 and 24% are shown in Fig. 2. The refractive index of the sugar solution was calculated with [15]. As expected, in the region of the central wavelength of the FBG (zone A), where the four curves overlap, the reflectivity at the Bragg wavelength is not affected by the variation of the refractive index. In contrast, in each of the curve shoulders (zones B and C), the reflectivity changes as a function of the refractive index. In other words, the SMSR of the FBG varies with the refractive index. The SMSR of the FBG as a function of the refractive index of the solutions is shown in Fig. 3. An optical variation of 4.2 dB was observed for concentration ranging from zero to 24% and the refractive index ranging from 1.3119 to 1.3601. Therefore, the sensitivity is higher than 87 dB/RIU. The simulation result from Eq. (6) is also shown in Fig. 3, which is in good agreement with the experimental result.

Besides the high sensitivity, the new sensor has two special characteristics. The first is that the measurement of the refractive index is not affected by the optical losses in the optical path of the sen-

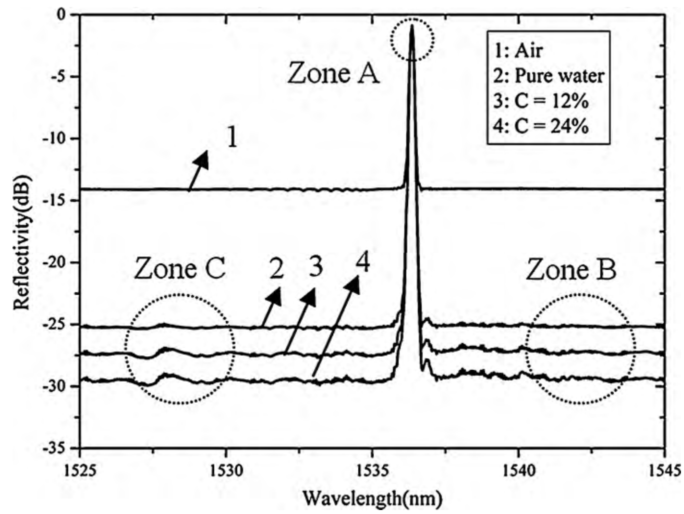

Fig. 2. Reflected spectral response of the sensing system immersed in different liquids of refractive index. The reflectivity at the central wavelength of the FBG (zone A) is not affected by the variation of the refractive index. In contrast, the reflectivity at each of the curve shoulders (zones B and C) changes as a function of the refractive index. That means the SMSR of the FBG varies with the refractive index.

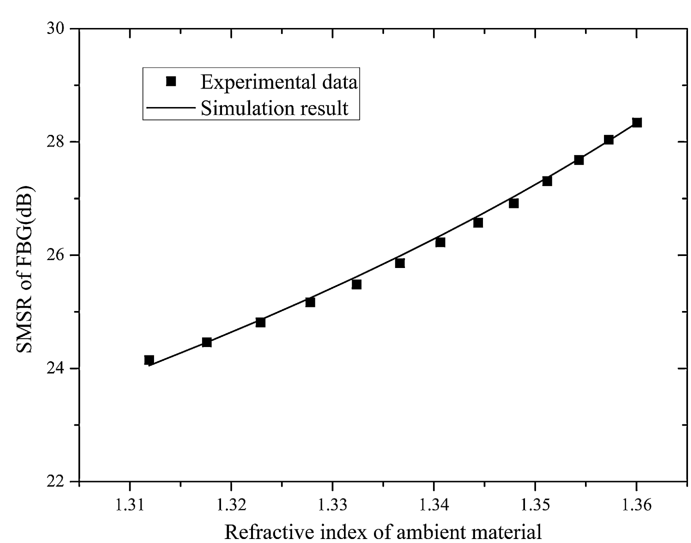

Fig. 3. Plot of change in SMSR of the FBG as a function of refractive index, simulated with Eq. (6). All of data are measured at the temperature of 25 °C and the wavelength of 1536.36 nm.